A whispering gallery mode strain sensor based on microtube resonator*

LIU Yu (刘宇), **YANG Hui-hui** (杨慧慧), **LU Yong-le** (路永乐)**, **DI Ke** (邸克), **and GUO Jun-qi** (郭俊启)
China Chongqing Engineering Research Center of Intelligent Sensing Technology and Microsystem, Chongqing University of Post and Telecommunications, Chongqing 400065, China

(Received 22 April 2020; Revised 15 May 2020)

A novel whispering gallery mode (WGM) strain sensor based on microtube has been proposed, where perceiving strain variations are reported via the dynamical regulation of a whispering gallery mode. The WGMs in the microtube resonator were evanescently excited by a micro-nano fiber fabricated by the fusion taper technique. The structural changes of microtubes under axial strain were simulated with finite element software, and the effect of microtube wall thickness on strain sensitivity was systematically studied through experiments. The experimental results show that the strain sensitivity of thin-walled microtube is found to be 1.18 pm/με and the *Q*-factor in the order of 4.4×10^4. Due to its simple fabrication and easy manipulation as well as good sensing performance, the microtube strain sensor has potential applications in high-sensitivity optical sensing.

Document code: A **Article ID:** 1673-1905(2021)04-0199-6
DOI https://doi.org/10.1007/s11801-021-0069-7

In the past few decades, strain sensors have been widely applied in many scientific and engineering fields, such as biomedical treatment, infrastructure monitoring, smart skin of robotic, etc[1-3]. In contrast to traditional strain sensors, optical fiber strain sensors have the advantages of small size, high precision and anti-electromagnetic interference. As a result, abundant research has been carried out on fiber optic strain sensors. Strain sensor based on fiber Bragg gratings (FBGs)[4,5] is one of the main research directions due to the mature and straightforward manufacturing process. However, sensors based on fiber gratings faced with the problems of strain sensitive effect, poor stability, and greatly affected by temperature. Besides, strain sensors based on the fiber interferometers, such as Fabry-Perot interferometers (FPIs)[6,7] and Mach-Zehnder interferometers (MZIs)[8,9], are also a significant research field with the advantage of the compact and miniaturized structure. But the sensing element of fiber interferometers fabrication complexity and expensive. Recently, with the continuing improvement of micro-nano structure photonic device, the strain sensor based on the whispering gallery mode (WGM), has become a popular research point because of the advantages of high quality factor (*Q*), small mode volume and simple preparation[10,11].

The WGM resonances are highly sensitive to the morphological changes of the resonator, changing of resonator size, shape, or refractive index will result in resonance wavelength shift or broadening and affect the coupling efficiency. On the contrary, the WGM shift can be monitored to reflect the changes in the surrounding environment of the microcavity. At present, spherical[12], bubble[13], or cylindrical[14-16] resonators produced by silica and polymer materials are commonly used for WGM strain sensors. Typically, micro-nano fiber is used to coupling resonators as the propagation constants of the micro-nano fiber will always be best matches that of most low-order radial modes of WGMs, which has a high coupling efficiency. For the strain sensor based on WGM, the precise alignment of coupling positions is an essential condition for stable high-efficiency coupling between the micro-nano fiber and the resonant cavity. However, two degrees of freedom must be considered for spherical symmetric resonators to achieve accurate alignment of the coupled micro-nano fiber to the resonator. In comparison, the cylindrical resonator with only one freedom can reduce the difficulty of precise alignment, and further reducing the impact on coupling efficiency, which limited the practical application of spherical or bubble-shaped resonators for strain sensing. For the advantage of the cylindrical resonator, Kavungal et al proposed a WGM strain sensor formed by a polymer-wire cylindrical resonator in 2017[15]. The strain sensitivity of the strain sensor is only 0.68 pm/με, and the *Q* factor is about 10^3. Subsequently, Kavungal et al. designed involves an inline cascade of optical micro-resonators (ICOMRs) coupled to multiple tapered sections along a single optical fiber in 2019[16], and

* This work has been supported by the National Key R&D Program of China (Nos.2018YFF01010202 and 2018YFF01010201), the National Natural Science Foundation of China (Nos.61705027 and 11704053), and the Basic Research Project of Chongqing Science and Technology Commission (Nos.CSTC-2017csmsA40017 and CSTC-2018jcyjax0619).
** E-mail: luyl@cqupt.edu.cn

the strain sensitivity of the sensor reaches 1.4 pm/με. However, the structure of ICOMRs is too complicated for practical application.

In this paper, a novel WGM strain sensor based on microtube resonator was proposed, which improved the sensitivity and reduced the structural complexity of the strain sensor. To reduce the structural complexity of the strain sensor, the silica capillary was used to construct the resonant cavity, and the WGMs in the microtube resonator were evanescently excited by a micro-nano silica optical fiber. However, the sensitivity of the strain sensor is influenced by many factors, and the thickness of the microtubule wall is one of the most critical factors. Therefore, this paper systemically studies the effects of different microtube wall thickness on the sensitivity of the sensor. The experimental results show that the Q factor of microtube resonator can reach 4.4×10^4, the sensitivity of the strain sensor can reach 1.18 pm/με, and the WGMs of microtube resonator can be tuned over the spectrum with a tuning range of ~3.54 nm.

The sensing principle of the sensor is based on the measurement of the spectral shift of the WGM resonances excited in the microtube resonator as a result of changes in its diameter due to the applied axial strain. The light wave propagates in micro-nano fiber produces a larger intensity evanescent field with the micro-nano fiber as the axis. When the distance between the micro-nano fiber and the microtube is relatively close, the light is coupled into the microtubule resonator in the form of evanescent waves, and the light wave of specific wavelength has a total reflection on the inner wall of the microtube. For the light wave satisfying the resonance condition, it will always propagate in the microtubule resonator resulting in the appearance of the spectral dips in the transmission spectrum of the coupled fiber taper. Under the influence of strain or stress continuously applied in the axial direction, both the diameter and refractive index of the microtube change, resulting in a spectral shift of WGM resonances.

In order to clearly show the distribution of stress and strain when the microtube is stretched, the mathematical model of microtube was established by finite element software ANSYS. The strain applied in the axial direction of the microtubule is 2 500 με, and Fig.1(a) shows the strain distribution in the axial direction of the microtube, and Fig.1(b) shows the radial strain distribution in the microtube. as can be seen from the figure, the diameter of microtube cavity is decreased.

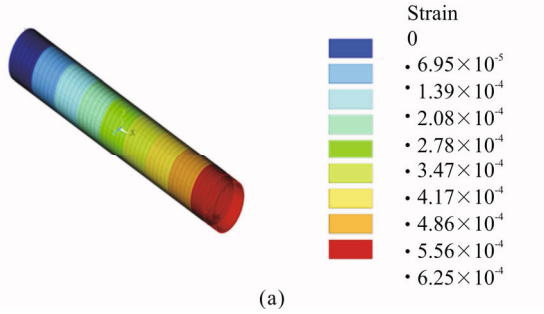

(a)

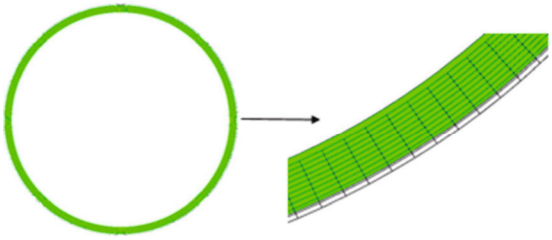

(b)

Fig.1 (a) Strain distribution in the axial direction of the microtube; (b) The microtube diameter changes when the strain applied to the microtube is 2 500με

The deformation and stress of microtube caused by applied strain will result in a shift of the WGMs[12-16], and the ratio of change in the wavelength of the WGMs $\Delta\lambda/\lambda$ can be represented as follows:

$$\frac{\Delta\lambda}{\lambda}=\frac{\Delta D}{D}+\frac{\Delta n}{n}\ , \tag{1}$$

where represent the change ratio of in the microtube diameter (D) caused by the deformation of the microtube, and represent the ratio of change in the refractive index (n) cause by the strain-optic effect[14,15].

For the microtube, the ratio of the transverse deformation and the axially applied tensile strain is Poisson's ratio (κ), and κ can be expressed as follows:

$$\kappa=-\frac{\Delta D/D}{\Delta L/L}, \tag{2}$$

where ΔL is the elongation length and L is the length of the microtube.

The change of microtubule diameter can result in material density alteration, and further cause the change of refractive index (n). Change of refractive index (Δn) can be expressed as:

$$\Delta n=-nP_{\text{eff}}\frac{\Delta L}{L}\ , \tag{3}$$

where P_{eff} is the effective strain-optic coefficient[14,15].

Therefore, the ratio of change in the wavelength of the WGMs $\Delta\lambda/\lambda$ can be further expressed as:

$$\frac{\Delta\lambda}{\lambda}=-\left(\kappa\frac{\Delta L}{L}+P_{\text{eff}}\frac{\Delta L}{L}\right)\ , \tag{4}$$

where the negative sign shows that the axial tensile strain applied to the micro-tube resonator will result in WGM resonance peak shifted toward the shorter wavelength.

In the experiment, the micro-nano fiber was used to excite WGM in the microtube efficiently. For the fabrication of the micro-nano fiber, a single-mode telecommunication optical fiber (SMF28, Coring) with the core diameter of 8.3 μm and the cladding diameter of 125 μm was selected, which was used to prepared the micro-nano fiber by the fused biconical taper method[17]. And the waist diameter and waist tapered of fabricated micro-nano fiber are about 2 μm and 6 mm, respectively. The material of micro-tubes is a flexible silica capillary tube (TSP075150, Polymicro Technologies), and the

inner diameter of the capillary was 74 μm, the wall thickness without coating was 26 μm. The micro-tubes wall thicknesses range from 5 μm and 25 μm were prepared by HF solution corrosion, to study the effect of micro-tubes with different wall thicknesses on the sensitivity of strain sensing.

The schematic diagram of the microtube strain sensing system is given in Fig.2. The two ends of the microtube were fixed on a micro-displacement platform, and the micro-nano fiber was coupled with the microtube resonator by high precision adjusted the displacement platform. The input port of the micro-nano fiber was connected to the broadband amplified spontaneous emission (ASE) light source (Fiber-Lake 1 600 nm ASE Light Source, wavelength range from 1 540 nm to 1 640 nm), while the output port connect with an optical spectrum analyzer (OSA) (AQ6370D, wavelength range from 600 nm to 1 700 nm) with 0.02 nm spectral resolution for real-time monitoring of the transmission spectrum. The platform 1 was fixed, and the axial strain was applied to the microtube by high-precision continuously moving micro-displacement platform 2. Assuming the length of the microtube fixed by platform 1 and platform 2 is L, and the axial change of the microtube is ΔL.

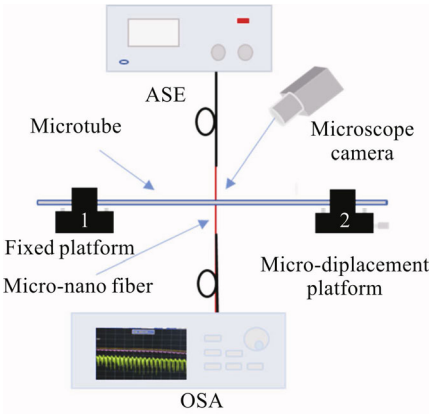

Fig.2 Experimental setup for the microtube strain sensing test system

The axial strain was applied to the microtube resonator by moving the platform 2 with 50 μm in the direction of away from platform 1. In the experiment, the fixed microtube length L is 20 cm, which corresponds to an axial strain of $\varepsilon=\Delta L/L=250\mu\varepsilon$. In order to prevent the interference of the temperature to the strain sensor, all the measurements were completed at a constant laboratory temperature of 20 °C.

Fig.3 shows the transmission spectrum of the micro-tube coupled with the micro-nano fiber. In the wavelength range of 1 540—1 610 nm, the Q factor and the average free spectral range (FSR) of the microtube resonator are 5.6×10^4 and 4.38 nm, respectively. In Fig.3, there is some stable low-order radial mode in the transmission spectrum. The relatively high transmission losses at the resonator peak are the coupling losses, which is caused by the coupled the light transmitted of the micro-nano fiber into the microtube. The remaining losses are the bending loss of the micro-nano fiber and the scattering losses caused by the uneven surface of the microtube. Since the microtube has a central hole, it has good flexibility and elastic characteristics compared with the cylindrical resonator[15,16].

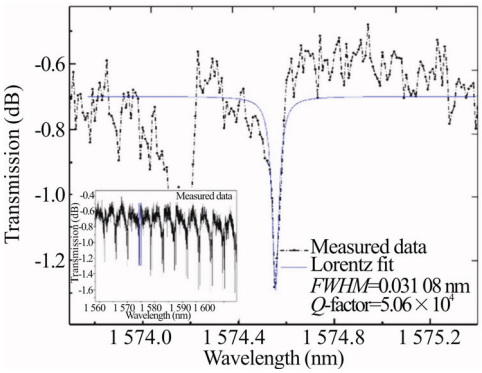

Fig.3 The transmission spectrum of the micro-nano fiber coupled with microtube resonator

Fig.4 shows the shift of the WGM transmission spectrum under different strain. The length of the microtube in this experiment was 20 cm, the inner diameter was 74 μm, and each time the strain is applied to the microtube resonator axially by moving the translation platform 2 with a step of 50 μm (corresponding to an axial strain of 250 με) in a direction away from the fixed platform 1, with the spectrometer recorded data spectrum once, and the axial strain increases from 0 to 1 750 με.

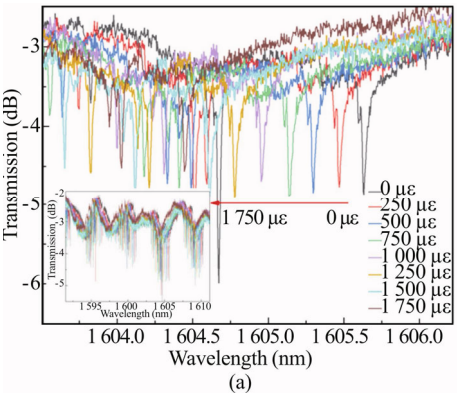

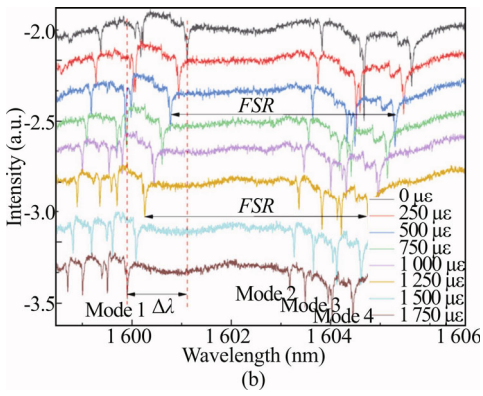

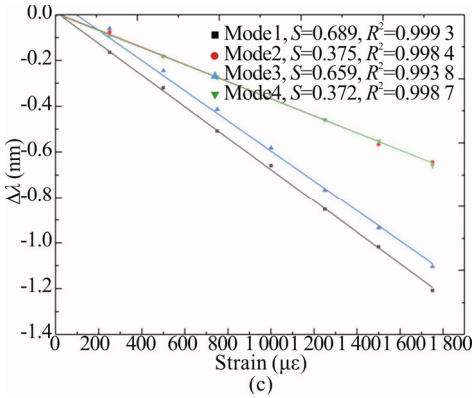

Fig.4 (a) WGM transmission spectrum shift with different strains; (b) Evolution of resonant spectrum in one *FSR* upon an increased strain; (c) The relationship between the WGM shift of different radial modes and applied axial strain for the case in (b)

It can be seen from Fig.4(a) that as the axially applied strain of the microtube increases continuously, the WGM resonance shifts towards shorter wavelength. And the intensity of WGM resonance changes only slightly in different strains. It is observed that the whispering gallery mode wavelength is shifted linearly from 1 601.11 nm to 1 599.90 nm over an elongation length of 350 μm. The *FSR* of the whispering gallery modes is 4.50 nm, and the *Q*-factor is about 8.0×10^4. Fig.4(b) shows the evolution of the resonance spectrum with increasing strain. It shows that when the WGM in the microtube resonator was excited by the micro-nano fiber, there are multi-order radial modes in the range of *FSR*. The trend of mode spacing narrowing upon increased strain is clearly shown in the figure, additional mode splitting appears in the WGM spectra, possibly due to strain-induced deformations and deviation of the resonator from its cylindrical shape[18]. Fig.4(c) shows the relationship between the WGM shift of different radial modes and applied axial strain for the case shown in (b). The slopes of the wavelength shift of mode1, mode2, mode3, and mode4 are 0.689 pm/με, 0.375 pm/με, 0.659 pm/με, and 0.372 pm/με, respectively. And the value of each slope represents the strain sensitivity corresponding to each whispering gallery radial mode. According to the value of R^2, the strain sensing response based on the WGM microtube has a good linear fit.

In the coupling experiment of microtube resonator and micro-nano fiber, the length of the microtube was 20 cm, which can sustain an axial elongation of 0.6 mm to 0.65 mm, and the corresponding axial strain is 3 000με—3 500με. When the applied strain exceeds the range, the chance of breakage of the microtube is increased. Different strain are applied to the microtubules to adjust the WGM wavelength position. The whispering gallery modes are selected for tracking the wavelength shift, and it can be seen that mode1 has a maximum shift of Λ=3 500με×0.689 pm/με=2.412 nm, which allow us to tune WGMs over half a free spectral range. which allows tuning WGMs spectral shift occurred within the *FSR* range of the spectrum to avoid ambiguity in identifying the location. Relative to the non-strain mode, it is also important to avoid sequential changes in the modal components caused by strain-induced microtube deformation[19].

According to theoretical analysis, the sensing sensitivity of the microtube is related to its shape and size. The influence of different wall thicknesses on strain sensing sensitivity will be analyzed below. In the experiment, the inner diameters of the microtubes were all 74 μm, and the wall thicknesses were 25 μm, 9.6 μm, 9.3 μm, and 6.6 μm, respectively. With the strain increases Fig.5 shows the wavelength shifts of the highest intensity WGM with axial elongation of these microtubes with the same inner diameter and different wall thicknesses. The mode spacing can be observed to increase in the gain region with the decreasing size of the microtube resonator thickness. It is also found that the thinner-walled thickness microtubes are more flexible and have good elastic characteristics when compared with thicker-walled thickness microtubes. In the experiment, the axial strain range of thin-walled microtubes was 2 500με—3 000με, which is smaller than that of thick-walled microtubules. This is due to the corroded microtubules is not deformed uniformly when they are elongated in the axial direction.

Fig.6 shows the response curves of strain sensitivity. The wall thickness of microtubules was 25 μm, 9.6 μm, 9.3 μm, and 6.6 μm, respectively. For different wall thicknesses, the radial mode with maximum shift was selected. The strain sensing sensitivity of this mode is 0.672 pm/με and 0.880 pm/με, 1.02 pm/με, 1.18 pm/με, respectively. It can be seen from Fig.7 that as the thickness of the microtube decreases, the strain sensitivity of the microtube strain sensor gradually increases. The whispering gallery modes of the microtube with the wall thickness of 6.6 μm have been tuned over the spectrum with the tuning maximum range of 3.54 nm. Therefore, when designing a WGM strain sensor based on a microtube resonator, we can choose a microtube with a thinner wall thickness as the sensor device, which can improve the sensitivity of the microtube.

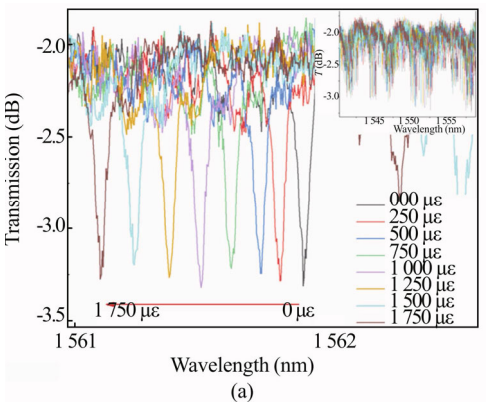

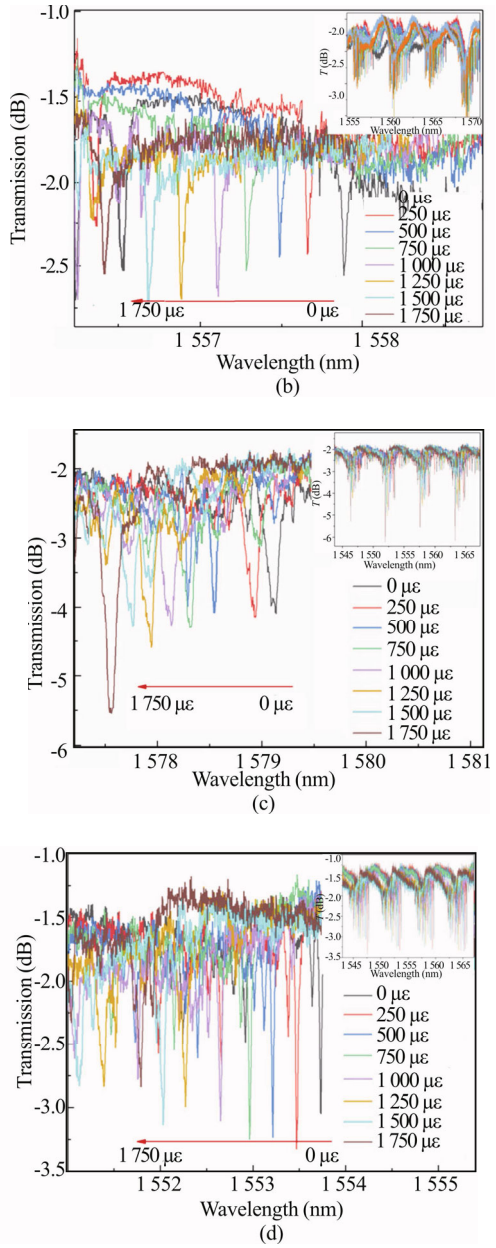

Fig.5 Strain transfer spectra when the microtube wall thickness is (a) 25 μm, (b) 9.6 μm, (c) 9.3 μm, (d) 6.6 μm

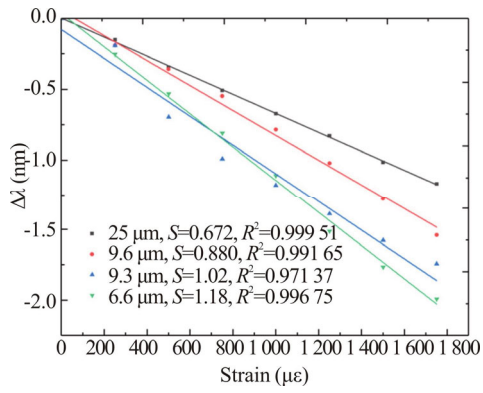

Fig.6 Strain sensitivity of microtubes with different wall thicknesses

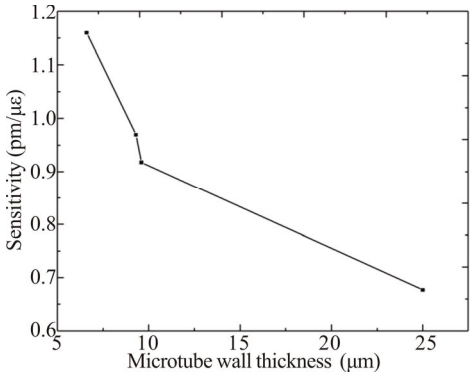

Fig.7 The relationship between strain sensitivity and microtube wall thickness

In conclusion, a WGM strain sensor based on microtube resonator is proposed, which improves the sensitivity and reduces the structural complexity of the strain sensor. The WGMs in the microtube resonator were evanescently excited by a micro-nano fiber fabricated by the fusion taper technique. As the axial strain is continuously applied to the microtubules, the WGMs are shifted linearly towards the shorter wavelength side. This paper studied the effect of microtube wall thickness on the sensitivity of strain sensing systematically. The strain sensitivity of the thin-walled microtubes is found to be 1.18 pm/με and the Q-factor in the order of 4.4×10^4, which can be tuned over the spectrum with a tuning range of ~3.54 nm. The simple and low-cost strain sensor has considerably potential applications, especially in the field of high-precision strain sensing.

References

[1] R. H. Kim, D. H. Kim, J. Xiao, B. H. Kim, S. I. Park, B. Panilaitis, R. Ghaffari, J. Yao, M. Li, Z. Liu, M. Viktor, D. G. Kim, A. Le, G. Ralph, L. David, Kaplan, G. O. Fiorenzo, Y. G. Huang, K. Zhan and A. R. John, Nature Materials **9**, 929 (2010).

[2] T. Yamada, Y. Hayamizu, Y. Yamamoto, Y. Yomogida, A. Izadi-Najafabadi, D. N. Futaba and K. Hata, Nature Nanotechnology **6**, 296 (2011).

[3] Q. Hua, J. Sun, H. Liu, R. Bao, R. Yu, J. Y. Zhai and Z. L. Wang, Nature Communications **9**, 1 (2018).

[4] L. Zhang, Y. Liu, X. Gao and Z. Xia, Applied Optics **54**, 109 (2015).

[5] C. E. Campanella, A. Cuccovillo, C. Campanella, A. Yurt and V. Passaro, Sensors **18**, 3115 (2018).

[6] M. S. Ferreira, P. Roriz, J. Bierlich, J. Kobelke, K. Wondraczek, C. Aichele, K. Schuster, J. L. Santos and O. Frazão, Optics Express **23**, 16063 (2015).

[7] C.Yin, Z. Cao, Z. Zhang, T. Shui, R. Wang, J. Wang, L. Lu, S. L. Zhen and B. L. Yu, IEEE Photonics Journal **6**, 1 (2014).

[8] H. Y. Choi, M. J. Kim and B. H. Lee, Optics Express **15**, 5711 (2007).

[9] L. Men, P. Lu and Q. Chen, IEEE Photonics Technology

Letters **23**, 320 (2011).

[10] L. He, S. K. Özdemir, J. Zhu, W. Kim and L. Yang, Nat. Nanotechnol. **6**, 428 (2011).

[11] C. Ciminelli, G. Brunetti, F. Dell'Olio, F. Innone, D. Conteduca and M. N. Armenise, Rigorous Design of an Ultra-High Q/V Photonic/Plasmonic Cavity to Be Used in Biosensing Applications, In International Conference on Applications in Electronics Pervading Industry, 185 (2016).

[12] T. Ioppolo, M. Kozhevnikov, V. Stepaniuk, M. V. Ötügen and V. Sheverev, Applied Optics **47**, 3009 (2008).

[13] R. Henze, T. Seifert, J. Ward and O. Benson, Optics Letters **36**, 4536 (2011).

[14] C. L. Linslal, M. Kailasnath, S. Mathew, T. K. Nideep, P. Radhakrishnan, V. P. N. Nampoori and C. P. G. Vallabhan, Optics Letters **41**, 551 (2016).

[15] V. Kavungal, G. Farrell, Q. Wu, A. K. Mallik and Y. Semenova, Journal of Lightwave Technology **36**, 1757 (2017).

[16] V. Kavungal, G. Farrell, Q. Wu, A. K. Mallik, C. Shen and Y. Semenova, Optical Fiber Technology **50**, 50 (2019).

[17] S. Liu, C. R. Liao and Y. P. Wang, Journal of Applied Sciences **36**, 104 (2018). (in Chinese)

[18] M. Hossein-Zadeh and K. J. Vahala, Optics Express **14**, 10800 (2006).

[19] W. V. Klitzing, R. Long, V. S. Ilchenko, J. Hare and Valérie Lefèvre-Seguin, Optics Letters **26**, 166 (2001).